

CHEMICAL FRACTIONATION IN TITANIFEROUS CLINOPYROXENE FROM BAYUDA, SUDAN

DAVID C. ALMOND

Department of Geology, Faculty of Science, University of Kuwait, P.O. Box 5969, 13060 Safat, Kuwait

ABSTRACT

Clinopyroxene in basanites and their late residual fractions from the Bayuda Desert, Sudan, shows initial trends of enrichment in Al and Ti accompanied by decline in Si and the ratio of Mg to Fe. During the second stage of fractionation (confined to small volumes of residual magma), there was little variation in Mg/Fe, but a continued increase in Al and Ti led to peak values of more than 11 wt.% Al_2O_3 and 6% TiO_2 . Hourglass zonation is characteristic of this stage. A third and final stage is marked by a complete change, toward iron enrichment and lower levels of Al and Ti. Although the late residuals from which these pyroxenes crystallized were highly alkaline, there is only negligible increase in the aegirine component. Textures indicate that the third stage began abruptly, and the mineralogical variations seem to require an increase in ferri-/ferrous ratio in the system at that point.

Keywords: pyroxene, titanian augite, basanite, hourglass zoning, oxygen fugacity, Bayuda desert, Sudan.

SOMMAIRE

Le clinopyroxène des basanites (et de leurs fractions différenciées) du désert de Bayuda (Soudan) montre un enrichissement initial en Al et Ti, accompagné d'un appauvrissement en Si et dans le rapport de Mg à Fe. Au cours du second stade du fractionnement, qui porte sur des volumes restreints de magma résiduel, il y a eu très peu de variation en Mg/Fe; par contre, Al et Ti ont continué à augmenter, pour atteindre plus de 11% Al_2O_3 et 6% TiO_2 (en poids). Une zonation en sablier est typique de ce stade. Le troisième et dernier stade de croissance montre un changement radical, vers un enrichissement en fer et des teneurs plus basses en Al et Ti. Quoique les fractions résiduelles desquelles ces pyroxènes ont cristallisé étaient fortement hyperalkalines, il n'y a pas d'enrichissement important dans le pôle aegyrine. D'après les textures, le dernier stade aurait débuté soudainement; les variations minéralogiques semblent indiquer une augmentation subite du rapport de Fe^{3+} à Fe^{2+} du système.

(Traduit par la Rédaction)

Mots-clés: pyroxène, augite titanifère, basanite, zonation en sablier, fugacité d'oxygène, désert de Bayuda, Soudan.

INTRODUCTION

Pyroxene in basanitic volcanic rocks from Bayuda, Sudan, shows extensive internal fractionation, par-

ticularly where there has been local segregation of late-stage, syenitic liquids. The Bayuda pyroxene trend, initially similar to that in other strongly alkaline provinces, diverges notably from trends in mildly alkaline and tholeiitic suites. However, its final stage is characterized by iron enrichment and the reversal of earlier trends, so that the last pyroxene is much nearer to those in mildly alkaline and tholeiitic suites. This paper defines these chemical variations using electron-microprobe and whole-rock analytical data.

GEOLOGICAL SETTING

The pyroxene suite described here occurs in alkali basaltic rocks of Jebel Hiwaysh ($32^{\circ}15'E$, $17^{\circ}36'N$), one of about one thousand small volcanoes in the Bayuda desert of northern Sudan (Fig. 1). The petrography and chemistry of the volcanic rocks have been described by Almond *et al.* (1984), following earlier work by Barth & Meinhold (1979) and Almond *et al.* (1969). Volcanicity was intermittent from Late Cretaceous to Recent and was characterized by the association basanite - nepheline hawaiite - nepheline benmoreite - phonolite, although only the first two of these rock types are abundant. In the older fields, all that remains of the original vol-

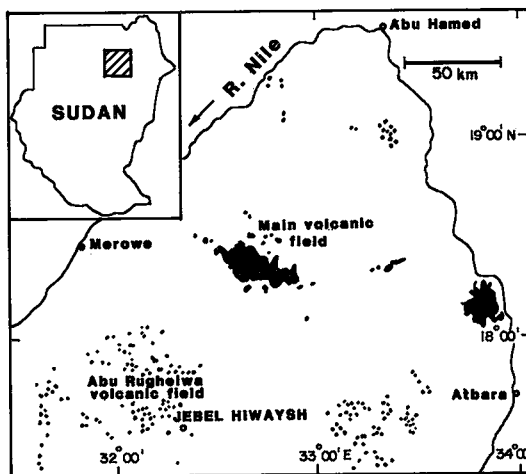


FIG. 1. Location of Jebel Hiwaysh within the Bayuda Desert of north-central Sudan, and its relation to other Cretaceous and Cenozoic basaltic rocks in this region.

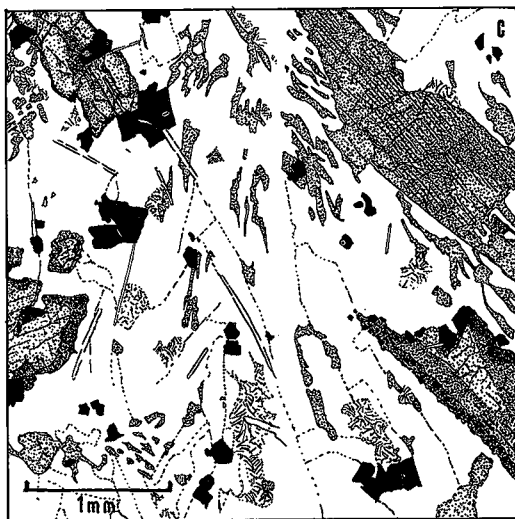
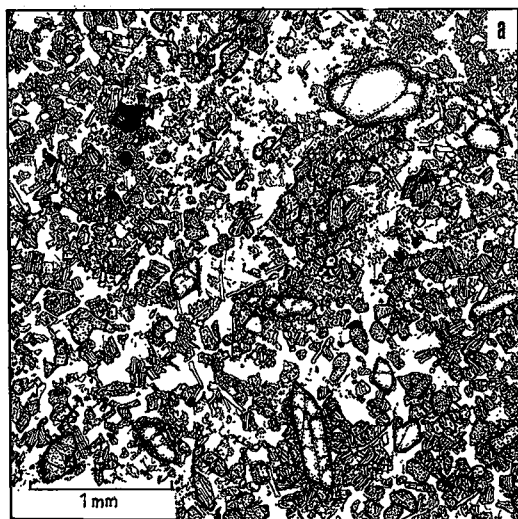


FIG. 2. Petrographic drawings of the host rocks. (a) Sparsely porphyritic basanite. Most of olivine (shown with heavy outlines) is in phenocrysts, whereas most pyroxene (fine stipple) is in groundmass granules. Rare pyroxene phenocrysts occur elsewhere in this rock. (b) Augite-olivine-phyric teschenite. Augite (fine stipple) shows zoning in phenocrysts, with outer margin similar in composition to groundmass augite grains. The section also contains plagioclase (laths), olivine (clear, with heavy outlines) and magnetite (black). (c) Coarse segregation in teschenite. Large, prismatic augite (stippled) with hourglass zoning commonly shows an outer rim of pale green pyroxene enclosing magnetite (bottom right). The smaller, irregular pyroxene grains in the central area are also pale green and are partly intergrown with sanidine.

canoes are isolated necks interspersed with remnants of lava flows and cinder beds. Jebel Hiwaysh is unusual in that during its activity the substructure was intruded by a near-vertical ring-dyke, 1.6 km in diameter, concentric with the central neck and only a few meters wide. Both dyke and neck are composed of teschenite, and the dyke also contains diffuse, relatively coarse-grained segregations in patches.

The suite of pyroxenes described in this paper comes from basanite lava, teschenite of the central neck, and a coarse-grained segregation within the ring-dyke (Fig. 2). Plagioclase, clinopyroxene, olivine and titaniferous magnetite are the major constituents; sanidine and anorthoclase are additional major components of the segregation, and anorthoclase is found interstitially in basanite and teschenite. Natrolite and analcime are late-stage com-

ponents of the segregation, but the natrolite, at least, is considered to be an alteration product of nepheline. These rocks are fresh, except for partial chloritization of olivine in the segregations. Apatite is a common accessory mineral, and there are traces of kaersutite and biotite in the basanite.

Figure 2 illustrates the different textural relations of the pyroxene in the three host rocks. In the basanite, purplish brown clinopyroxene is largely a groundmass constituent, whereas the teschenite contains numerous augite phenocrysts zoned from a pale fawn core to a brown margin. The most prominent pyroxene grains in the coarse segregation are prismatic, up to 5 mm long, and display hourglass zonation. Much smaller, pale green anhedral grains are intergrown with sanidine; similar pyroxene also occurs as a sharply defined rim that overgrew and replaced some of the large prisms. The green pyroxene overgrowths generally contain an abundance of titaniferous magnetite grains. Judging from the distribution of these various phases, the final fraction of magma crystallized sanidine, nepheline, green pyroxene, a little olivine (Fo_{55}) and magnetite.

The basanite and teschenite have similar bulk compositions (Table 1). The coarse segregation is significantly richer in Si, Al and Na, and may be classified as feldspathoidal syenogabbro. It represents a fractionate from the teschenite magma, which underwent further internal fractionation, so that the final interstitial liquid reached the composition of a feldspathoidal syenite. It was from this last magmatic liquid that the green pyroxene crystallized.

FRACTIONATION TRENDS

Changes in pyroxene composition corresponding with the textural evolution are defined by representative microprobe analyses in Table 2, and are illustrated in three variation diagrams (Figs. 3, 4, 5). A plot of oxide components against evolutionary stages (Fig. 3) shows initial decreases in Si and Mg from phenocryst core toward the groundmass of the basanite and teschenite, compensated by increases in Al and Ti. The large, hourglass-zoned augite prisms extend these trends outward from a pale-colored core into the purple rim of their prism zones. Peak values reach more than 11 wt.% Al_2O_3 and 6% TiO_2 , whereas SiO_2 falls to less than 42%. On the other hand, basal sectors of the prisms record sharp and covariant reversals of these trends outward from the core, with rising Si values and modest decreases in Al and Ti. Chemical variation shows a progressive trend only if the reversal in the basal sector is included; otherwise there is a sharp compositional break between groundmass pyroxene and the core zone of the prisms.

Fractionation of Al, Ti and Si between prismatic and basal faces is the normal expression of hourglass zoning in augite. However, the volume ratio of prism to basal sectors in these particular crystals is about 8:1, so that the overall trend is relatively close to the variation shown by the prism sectors (indicated by a solid line in Fig. 3). Magnesium and total iron show only small variations at this stage; nevertheless, a discernible trend is shown by the ratio $Mg/(Mg + Fe + Mn)$, which continues to fall in the prism zone, but reverses to higher values in the basal sector (Table 2, columns 8 to 12).

On a conventional Ca-Mg-(Fe+Mn) compositional triangle (Fig. 4a), the trend from cores of phenocrysts in basanite to margins of prisms in the coarse patches rises steeply away from the Mg corner to well above the 50% Ca line. This trend is a feature characteristic of many other basanite provinces (e.g., Carmichael *et al.* 1974). The basanite trend is thus quite distinct from both the tholeiitic trend (e.g., Skaergaard) and mildly alkaline trend (e.g., Shiant Isles). Moreover, Figure 4 shows how the relatively compact cluster on the Ca-Mg-(Fe+Mn) diagram (Fig. 4a) opens out greatly once coherent variations in Al and Ti are taken into account (Fig. 4b).

TABLE 1. WHOLE-ROCK CHEMICAL COMPOSITIONS, BAYUDA SUITE

	1	2	3
Oxide weight percentages			
SiO_2	41.7	42.9	46.7
TiO_2	2.8	2.8	2.6
Al_2O_3	14.8	14.6	17.4
Fe_2O_3	2.0	2.0	2.5
FeO	10.5	10.9	7.3
MnO	0.2	0.2	0.2
MgO	10.6	10.3	3.7
CaO	11.0	10.9	8.8
Na_2O	3.9	2.9	6.6
K_2O	1.6	1.7	2.8
P_2O_5	0.8	0.9	1.3
FeO(det.)	8.7	8.14	6.12
ΣFe as Fe_2O_3	13.60	14.00	10.50
CIPW norms			
Q	-	-	-
Or	5.0	10.0	16.7
ab	-	3.4	13.1
an	18.1	21.6	9.7
lc	3.5	-	-
ne	17.9	11.5	23.0
di	25.5	22.3	21.6
ol	19.9	21.1	4.2
mt	3.0	3.0	3.7
il	5.3	5.3	5.0
ap	2.0	2.0	3.0

1. Basanite from lava on inner side of ring dyke, Jebel Hwaysh.
 2. Teschenite intrusion into lavas of Jebel Hwaysh.
 3. Segregation within teschenite ring-dyke.
- The samples were analyzed by XRF using a Philips PW1410 X-ray spectrometer in the Department of Geology, Portsmouth Polytechnic, England. Analyst: S. Pooler. The XRF oxide determinations have been recalculated to 100%, and Fe_2O_3 standardized according to the conventions of Thompson *et al.* (1972). A separate determination of FeO by wet chemistry was also carried out, and is shown as FeO(det.).

Coherency of Al and Ti substitution in pyroxenes of alkaline rocks has often been remarked upon (e.g., Le Bas 1962, Verhoogen 1962, Yagi & Onuma 1967), and the pattern of Al:Ti distribution shown in Figure 5 is typical. The points plot along an almost straight line at a lower Ti level than the 2 Al:Ti line, along which all points would lie if variations were attributable exclusively to the hypothetical titaniferous pyroxene component $CaTiAl_2O_6$ (cf. Scott 1980). The excess of Al over this ratio (Fig. 5) is attributed to the Ca-Tschermaks component ($CaAl_2SiO_6$).

Sharp compositional changes mark the incoming of green pyroxene, which overgrew and partly replaced some of the hourglass prisms and which forms delicately branched grains intergrown with sanidine. In such end-stage pyroxenes, SiO_2 rises to over 52 wt.%, Al_2O_3 and TiO_2 fall to $\leq 1\%$, and total iron oxide increases to nearly 20%. These changes bring the trend back toward that of the Shiant Isles (Fig. 4). This late pyroxene at Bayuda is also similar in composition to "ferrosalite" described by Larsen (1976) from early augite syenite at Ilimaussaq, although the "ferrosalite" is reddish brown, not green.

Estimates of oxidation state based on pyroxene

TABLE 2. REPRESENTATIVE MICROPROBE DATA FOR CLINOPYROXENES FROM BASANITES OF JEBEL HIWAYSH, BAYUDA, SUDAN

	basanite phenocrysts				basanite groundmass			Segregation hourglass zonation				rim 13	groundmass 14	
	1	2	3	4	5	6	7	8 core	9 prism	10	11 base			12
oxide weight percentages														
SiO ₂	51.24	51.64	49.50	48.50	47.11	47.00	46.70	44.06	43.17	41.80	44.58	47.51	52.03	51.16
TiO ₂	1.40	1.23	1.73	2.15	3.06	3.29	3.42	4.66	5.57	6.12	4.57	3.59	0.56	0.35
Al ₂ O ₃	3.93	3.73	5.47	6.58	7.44	6.95	6.10	9.51	10.10	11.29	9.21	6.68	1.10	0.74
Cr ₂ O ₃	0.49	0.57	0.41	0.86	0.13	0.22	0.15	0.16	0.15	n.d.	n.d.	0.13	n.d.	n.d.
Σ FeO	5.98	6.26	6.89	6.44	6.82	8.03	9.25	8.37	8.40	8.85	8.42	8.05	13.09	19.86
MnO	n.d.	n.d.	0.14	n.d.	0.11	0.11	0.14	0.16	n.d.	n.d.	0.17	n.d.	0.35	0.56
MgO	15.21	14.61	14.04	13.21	12.52	12.12	11.05	9.85	9.36	8.78	9.78	11.14	10.02	5.54
CaO	21.36	21.58	21.81	22.26	22.15	22.58	22.34	22.56	22.76	22.51	22.83	22.90	22.14	20.61
Na ₂ O	0.38	0.39	n.d.	n.d.	0.66	n.d.	0.56	0.67	0.49	0.65	0.44	n.d.	0.71	1.14
Fe ₂ O ₃ (calc.)	0.00	0.00	0.07	0.00	1.76	0.27	1.14	1.36	0.00	0.98	0.00	0.00	0.27	0.90
FeO (calc.)	5.98	6.26	6.82	6.44	5.23	7.80	8.22	7.15	8.40	7.97	8.42	8.05	12.85	19.05
number of ions to six oxygen atoms														
Si	1.886	1.902	1.834	1.789	1.749	1.752	1.770	1.660	1.636	1.583	1.683	1.792	1.982	2.030
Al _z	0.114	0.098	0.166	0.202	0.251	0.248	0.230	0.340	0.364	0.417	0.317	0.208	0.018	-
Al _y	0.057	0.065	0.073	0.073	0.075	0.060	0.041	0.082	0.089	0.087	0.093	0.089	0.031	0.034
Ti ₄	0.039	0.034	0.048	0.060	0.085	0.093	0.087	0.132	0.159	0.174	0.130	0.102	0.016	0.010
Fe ³⁺	0.000	0.000	0.001	0.000	0.049	0.008	0.032	0.039	-	0.028	-	-	0.008	0.027
Cr	0.014	0.017	0.012	0.025	0.004	0.006	0.005	0.005	0.005	-	-	0.004	-	-
Mg	0.834	0.802	0.775	0.730	0.693	0.678	0.620	0.553	0.529	0.496	0.550	0.626	0.568	0.323
Fe ²⁺	0.184	0.193	0.213	0.199	0.163	0.245	0.259	0.225	0.266	0.252	0.266	0.254	0.409	0.624
Mn	-	-	0.004	-	0.004	0.004	0.005	0.005	-	-	0.005	-	0.011	0.029
Ca	0.842	0.852	0.866	0.884	0.881	0.908	0.902	0.911	0.924	0.914	0.924	0.925	0.904	0.865
Na	0.027	0.028	-	-	0.047	-	0.041	0.049	0.030	0.048	0.032	-	0.053	0.087
100Σ { Mg	44.83	43.44	41.69	40.23	38.72	36.79	34.10	31.91	30.77	29.35	31.52	34.68	29.89	17.29
Σ Fe + Mn	9.89	10.44	11.73	11.01	12.07	13.94	16.28	15.52	15.47	16.57	15.53	14.07	22.53	36.40
Ca	45.27	46.12	46.58	48.75	49.22	49.27	49.61	52.56	53.75	54.08	52.95	51.25	47.58	46.31
Mg/(Mg+ΣFe+Mn)	81.92	80.60	78.05	78.58	76.24	72.51	67.69	67.27	66.54	63.92	66.99	71.14	57.03	32.20

Analyses were made using an EDS system with Si(Li) detector in the Department of Earth Sciences, University of Cambridge, England. Procedure followed Sweetman & Long (1969); the raw data were processed by the method of Statham (1976). Compositions 1 to 4 refer to pale fawn-colored core of phenocryst in basanite and tschermite, whereas 5 and 7 refer to brown, prismatic grains in the groundmass, and 6 pertains to the overgrowth on a phenocryst. Compositions 8 to 12 illustrate hourglass zoning in large, prismatic crystals in a segregation, and show differences between pinkish purple prism sectors and paler basal sectors. Composition 13 pertains to a pale green rim on an hourglass-zoned prism, and 14, to a pale green grain associated with sanidine in the segregation matrix. Totals are 100% (recalculated). Estimates of Fe₂O₃ and FeO were obtained by the method of Neumann (1976).

stoichiometry (Neumann 1976) suggest that Fe³⁺/Fe²⁺ remains very low throughout the early stage of crystallization. It rises little in the late pyroxene, a conclusion in keeping with increased but still very low contents of Na (Fe³⁺ and Na are known to maintain approximate equality in most cases). On the other hand, where green pyroxene overgrew hourglass prisms, the former contains numerous small octahedra of titaniferous magnetite that become larger and more numerous toward the matrix, suggesting an increase in the ferric/ferrous ratio of the residual melt at this time.

Substitution of the aegirine component did not become significant until the final stages of fractionation, and even then the content of Na₂O exceeds 1% in only a few samples. This contrasts with much more extensive aegirine substitution characteristic of many alkaline suites, such as that at Shonkin Sag (Nash & Wilkinson 1979; Fig. 4a), in which Na enrichment of pyroxene is accompanied

by notable increase in the Fe³⁺/Fe²⁺ ratio and a sharp change in color and texture. The Bayuda suite shows similarly abrupt changes in texture and color, but the composition of the last fraction has greater affinity with tholeiitic and mildly alkaline trends than with strongly alkaline trends (Fig. 4a).

In the terminology of the "pyroxene quadrilateral", the early pyroxene compositions evolved from titaniferous diopside in the cores of phenocrysts to titanium-rich diopside with high Ca in groundmass grains. Trends such as this are common in basanite suites (e.g., Huckenholz 1973), and extreme compositions occur in the rim of phenocrysts of some Tahitian basalts. Tracy & Robinson (1977) have recorded up to 8.8% TiO₂ and 13.6% Al₂O₃ in rims; these values are exceeded only in pyroxene from lunar basalts. At Bayuda, the most extreme values, over 6% TiO₂ and 11% Al₂O₃, are found within the coarse-grained segregation. However, in the latest pyroxene fraction of this segregation, the contents

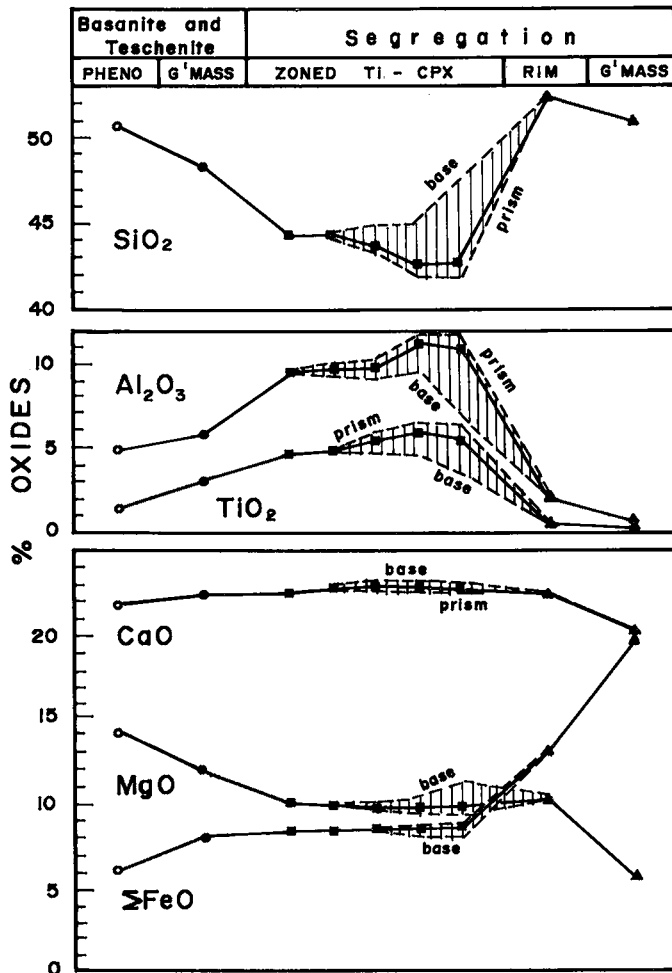


FIG. 3. Variation in some major oxides with evolutionary stage of the pyroxenes. The plot uses analytical data given in Table 2 plus some additional microprobe data. The symbols used for plotting points in each stage are also employed in subsequent figures. The vertically ruled areas indicate the approximate compositional differences between prism and basal sectors of hourglass-zoned crystals, whereas the solid line shows the variation in bulk composition.

of Ti and Al drop abruptly, and there is strong enrichment in Fe, so that the final trend is from diopside to Fe-rich diopside.

HOURGLASS ZONING

Trends in the early pyroxene of the coarse segregation (solid lines in Fig. 3) refer to average compositions corrected for the relative volumes of prism and basal sectors of the hourglass-zoned crystals. The basal sectors themselves show a reversal of the Al + Ti enrichment trend. Dowty (1976) offered an

elegant explanation of sector zonation based on the assumption that cation absorption into some proto-sites on the growing faces will favor small, highly charged ions (including Al, Ti and Fe^{3+}). In the case of augite, such sites are more numerous on the prism faces, so that rapid, metastable growth will enrich the prism sectors in these higher-field-strength ions. Sector zoning is a metastable phenomenon; Dowty hypothesized that *all* Ti, Al and Fe^{3+} may be incorporated as a result of metastable growth-processes. This extension seems unwarranted and cannot be supported by the incorrect supposition that

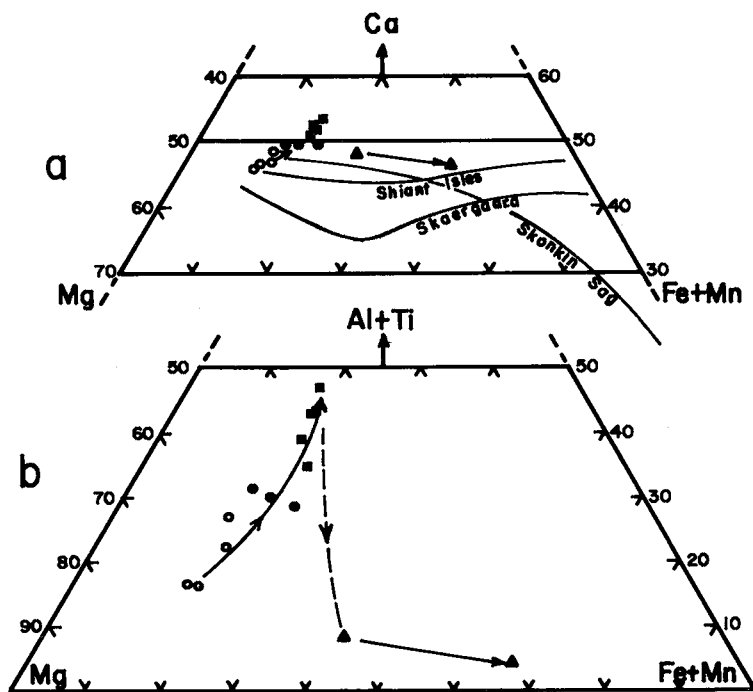


FIG. 4. (a) Pyroxene compositions plotted in part of the triangle Ca:Mg:(Fe+Mn), expressed in atomic proportions. Shiant Isles trend from Gibb (1973), Shonkin Sag trend from Nash & Wilkinson (1970), and Skaergaard trend from Wager & Brown (1967). (b) Variation in atomic Mg:(Fe+Mn):(Al+Ti) for the Bayuda suite of pyroxenes. Symbols as in Figure 3.

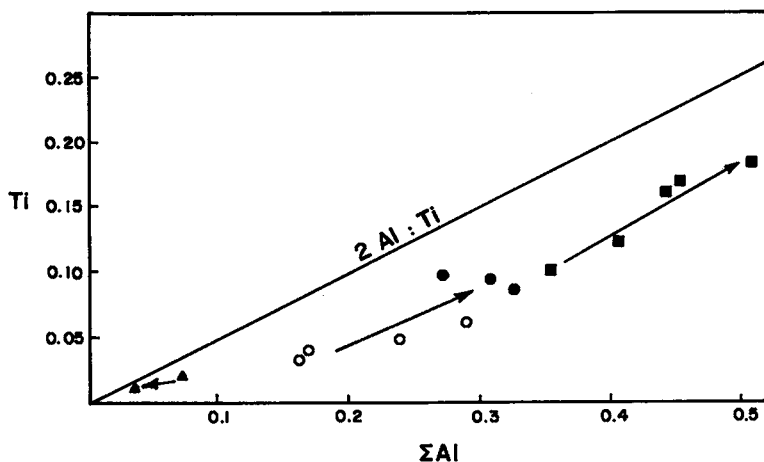


FIG. 5. Ratios of Ti vs. Al (atomic) in the Bayuda suite of pyroxenes. Symbols as in Figure 3.

"as a rule titanogites occur in volcanic rocks which are only mildly silica-undersaturated and moderately titanium-rich" (Dowty 1976, p. 468). It is also relevant that some examples of volcanic pyroxene from Tahiti show extreme enrichment in Al + Ti without sector zoning (Tracy & Robinson 1977). One may reasonably conclude that the metastable distribution of elements in sector zoning is superimposed on a general trend of increasing Al, Ti and, in some cases, Fe³⁺, and this general trend is in itself not necessarily metastable.

There is also a common, though not universal, connection between sector zoning and swallow-tail terminations in clinopyroxene. Wass (1973) attributed swallow-tail terminations in certain New South Wales pyroxene phenocrysts to rapid growth induced by quenching. The presence of swallow tails on some of the pyroxene grains in the Bayuda segregation cannot be the result of quenching but does suggest that relatively rapid growth of prism faces commonly accompanies development of hourglass zoning.

CONTROLS OF PYROXENE FRACTIONATION

In accounting for crystallization of (Al + Ti)-enriched clinopyroxene in highly alkaline magmas, most authors have appealed to fundamental traits in magma composition, particularly low contents of Si and Ti, acting in conjunction with low levels of oxygen fugacity. Low activity of silica is considered to have enhanced the uptake of Al, and therefore Ti, by increasing the stability of the silica-poor Ca-Tschermaks component (CaAl₂SiO₆) in pyroxene relative to the less silica-poor anorthite component (CaAl₂Si₂O₈) in plagioclase (Verhoogen 1962, Carmichael *et al.* 1970). Consequently, low activity of silica may delay the appearance of plagioclase until after olivine and clinopyroxene have been crystallizing for some time. Low activity of alumina, arising from an inherently Al-poor magma composition, may similarly inhibit plagioclase precipitation and cause large amounts of Al, some of it linked with Ti in the titaniferous pyroxene end-member, to enter pyroxene (Barberi *et al.* 1971). As an alternative, Gibb (1973) suggested that delayed crystallization of titaniferous magnetite could be a major reason for Ti (and hence Al) to enter pyroxene. Such delay might be ascribed to low fugacity of oxygen, the normal situation in internally buffered basic magmas of silica-undersaturated composition (Carmichael & Nicholls 1967). Reversals of these early trends are common, with Al and Ti falling back after their initial increase, and can be ascribed to the eventual incoming of plagioclase or titanian magnetite (or both). In the mildly alkaline Shiant Isles magma (Gibb 1973), this reversal occurred when the Mg/(Mg + Fe) value in the pyroxene fell to about

65%. In Bayuda, the reversal is delayed to the final stages, when the Mg value has fallen below 60%.

Many pyroxene sequences that include a reversal of the Al + Ti trend show a strong concomitant increase in the aegirine content, a feature said to reflect increased activity of Fe³⁺ in the liquid (Nash & Wilkinson 1970, Gibb 1973). Whereas iron enrichment of one kind or another generally characterizes the closing stages of pyroxene trends, it remains unclear to what extent oxygen fugacity determines the choice between final enrichment in ferrous iron leading toward hedenbergite *versus* the Na + Fe³⁺ trend toward aegirine.

The problem is to discern which of the postulated controls might have operated in Bayuda. The absence of plagioclase phenocrysts and sparseness of early magnetite suggest that, during initial fractionation, Al and Ti accumulated in the liquid and entered pyroxene in large amounts because crystallization of plagioclase and oxides was delayed by low silica activity and oxygen fugacity, respectively. The second stage of fractionation followed segregation of small amounts of liquid residue. These segregations were relatively impoverished in Mg and enriched in Si, Al, Na and K (see Table 1), compared with the parental magma, and doubtless also contained more volatiles. The single-step fractionation that produced these pockets thus resulted in a marked discontinuity in bulk composition. The pyroxene compositions record this discontinuity by a large compositional step, as does olivine (from Fo₇₀₋₇₇ in teschenite to Fo₅₀₋₆₀ in the segregations), and magnetite (from Fe:Ti 72:28 to 77:23). Moreover, a completely new feldspar assemblage appears. Around the margins of segregation pockets, early andesine gives way rapidly to sodic anorthoclase and is joined by sanidine and secondary natrolite, perhaps after nepheline. The large hourglass-zoned titanian augite is part of this new assemblage and, after the initial break, shows a continuation of the Al + Ti enrichment trend. The segregated magma was at this point crystallizing abundant feldspar and titaniferous magnetite. At first it seems difficult to explain the persistence of this trend; as can be seen from Table 1, however, the segregated magma was much richer in Al₂O₃ than the teschenite. This feature results from the delay in plagioclase precipitation. Moreover, the feldspar assemblage of the segregation is alkali-rich, and its crystallization would extract less Al than the plagioclase of the teschenite. Nor, apparently, did the continuing precipitation of titaniferous magnetite limit the simultaneous entry of Ti into pyroxene, perhaps because low oxygen fugacity restricted crystallization of iron (Table 2). There was, therefore, no immediate reversal of trend at this point, such as occurred in the Shiant Isles (Gibb 1973) and other mildly alkaline magmas. On the other hand, the steady decrease in the ratio

Mg/(Mg + Σ Fe + Mn), which characterized the initial pyroxene trend, came to a halt in the zoned grains of the segregate, reflecting the low magnesium content of the magma (Table 1, column 3).

In its final stage, pyroxene fractionation became dominated by iron enrichment, with reduced levels of Ca, Al and Ti. This trend involved ferrous iron, and is thus unlike that found in alkaline complexes in which pyroxene compositions became richer in aegirine at this stage. Controlling factors may have included preceding enrichment of the liquid in total iron, together with an increase in the ferric/ferrous ratio large enough to promote magnetite precipitation and the uptake of ferrous iron into pyroxene, but too small to allow a trend toward aegirine. All of this implies some change in the oxygen fugacity, which is likely to have been controlled to this point by internal buffering of the olivine + magnetite + silica-bearing magma (Nash & Wilkinson 1970). As silica activity in this undersaturated magma must have been very low, oxygen fugacity would have always lain below that of the fayalite - magnetite - quartz (FMQ) buffer, decreasing with falling temperature along a path parallel to that followed by FMQ itself. This trend would have continued as long as olivine and magnetite coexisted with a silica-bearing liquid (Nash & Wilkinson 1970). Even so, Carmichael *et al.* (1974) have made it clear that relationships between Fe^{3+}/Fe^{2+} and oxygen fugacity can be complex: Fe^{3+}/Fe^{2+} tends to be increased by increasing alkalinity, for example. However, all the obvious influences are expected to vary gradually, and so cannot account for the abruptness of the change toward iron enrichment recorded by the sharply defined and often replacive character of the late pyroxenes. The green pyroxene, with its enclosed octahedra of magnetite that rim some titanian augite prisms, is reminiscent of the pyroxene and magnetite seen around hornblende phenocrysts in many andesites. The pyroxene-magnetite assemblage presumably records some sudden change in the composition or availability of an accompanying volatile phase during eruption. In the case of the Bayuda pyroxenes, internal buffering of the oxygen fugacity by mineral phases and residual magma may have changed suddenly to external buffering by a volatile phase (Carmichael & Nicholls 1967). There are several ways in which this might happen. For example, Bailey (1980) has emphasized the dominance of CO_2 among volatiles related to alkaline magmatism. Rapid changes could reflect replacement of a CO_2 -rich volatile phase by a more oxygen- and water-rich mixture as a result of atmospheric contamination. Alternatively, the increased concentration of more oxidizing volatiles could be merely the result of their fractionation into the late residual fractions, but it is difficult to understand how this could have produced the sudden change required.

ACKNOWLEDGEMENTS

The microprobe analyses used in this paper were made with the generous help of Drs. J.V.P. Long and A. Buckley of the Department of Earth Sciences, University of Cambridge, in a laboratory supported partly by the National Environment Research Council. Many useful criticisms of the initial draft were provided by Prof. D.J. Shearman and Dr. D. O'Halloran. Mustafa Kambal of the University of Kuwait redrew the figures.

REFERENCES

- ALMOND, D.C., AHMED, F. & KHALIL, B.E. (1969): An excursion to the Bayuda volcanic field of northern Sudan. *Bull. Volc.* **33**, 549-565.
- , KHEIR, O.M. & POOLE, S. (1984): Alkaline basalt volcanism in northern Sudan - a comparison of the Bayuda and Gedaref areas. *J. Afr. Earth Sci.* **2**, 233-245.
- BAILEY, D.K. (1980): Volcanism, earth degassing and replenished lithosphere mantle. *Phil. Trans. R. Soc. Lond.* **A297**, 309-322.
- BARBERI, F., BIZOUARD, H. & VARET, J. (1971): Nature of the clinopyroxene and iron enrichment in alkalic and transitional basaltic magmas. *Contr. Mineral. Petrology* **33**, 93-107.
- BARTH, H. & MEINHOLD, K.D. (1979): Mineral prospecting in the Bayuda Desert. *Technical Report of the Sudanese German Exploration Project*. Bundesanstalt für Geowissenschaften und Rohstoffe, Hannover.
- CARMICHAEL, I.S.E. & NICHOLLS, J. (1967): Iron-titanium oxides and oxygen fugacities in volcanic rocks. *J. Geophys. Res.* **72**, 4665-4687.
- , ——— & SMITH, A.L. (1970): Silica activity in igneous rocks. *Amer. Mineral.* **55**, 246-263.
- , TURNER, F.J. & VERHOOGEN, J. (1974): *Igneous Petrology*. McGraw-Hill, New York.
- DOWTY, E. (1976): Crystal structure and crystal growth. II. Sector zoning in minerals. *Amer. Mineral.* **61**, 460-469.
- GIBB, F.G.F. (1973): The zoned clinopyroxenes of the Shiant Isles sill, Scotland. *J. Petrology* **14**, 203-230.
- HUCKENHOLZ, H.G. (1973): The origin of fassaitic augite in the alkali basalt suite of the Hocheifel area, western Germany. *Contr. Mineral. Petrology* **40**, 315-326.
- LARSEN, L.M. (1976): Clinopyroxenes and coexisting mafic minerals from the alkaline Ilimaussaq intrusion, South Greenland. *J. Petrology* **17**, 258-290.

- LE BAS, M.J. (1962): The role of aluminium in igneous clinopyroxenes with relation to their parentage. *Amer. J. Sci.* **260**, 267-288.
- NASH, W.P. & WILKINSON, J.F.G. (1970): Shonkin Sag laccolith, Montana. I. Mafic minerals and estimates of temperature, pressure, oxygen fugacity and silica activity. *Contr. Mineral. Petrology* **25**, 241-269.
- NEUMANN, E.-R. (1976): Two refinements for the calculation of structural formulae for pyroxenes and amphiboles. *Norsk Geol. Tidsskr.* **56**, 1-6.
- SCOTT, P.W. (1980): Zoned pyroxenes and amphiboles from camptonites near Gran, Oslo region, Norway. *Mineral. Mag.* **43**, 913-917.
- STATHAM, P.J. (1976): A comparative study of techniques for quantitative analysis of the X-ray spectra obtained with a Si(Li) detector. *X-ray Spectrom.* **5**, 16-28.
- SWEATMAN, T.R. & LONG, J.V.P. (1969): Quantitative electron-probe microanalysis of rock forming minerals. *J. Petrology* **10**, 332-379.
- THOMPSON, R.N., ESSON, J. & DUNHAM, A.C. (1972): Major element chemical variation in the Eocene lavas of the Isle of Skye, Scotland. *J. Petrology* **13**, 219-253.
- TRACY, R.J. & ROBINSON, P. (1977): Zoned titanian augite in alkali olivine basalt from Tahiti and the nature of titanium substitutions in augite. *Amer. Mineral.* **62**, 634-645.
- VERHOOGEN, J. (1962): Distribution of titanium between silicates and oxides in igneous rocks. *Amer. J. Sci.* **260**, 211-220.
- WAGER, L.R. & BROWN, G.M. (1967): *Layered Igneous Rocks*. Oliver & Boyd, Edinburgh.
- WASS, S.Y. (1973): The origin and petrogenetic significance of hour-glass zoning in titaniferous clinopyroxenes. *Mineral. Mag.* **39**, 133-144.
- YAGI, K. & ONUMA, K. (1967): The join $\text{CaMgSi}_2\text{O}_6 - \text{CaTiAl}_2\text{O}_6$ and its bearing on the titanaugites. *J. Fac. Sci. Hokkaido Univ., Ser. IV*, **13**, 463-483.

Received March 27, 1987, revised manuscript accepted December 10, 1987.